



CHORUS

This is the accepted manuscript made available via CHORUS. The article has been published as:

Peripheral nucleon-nucleon scattering at fifth order of chiral perturbation theory

D. R. Entem, N. Kaiser, R. Machleidt, and Y. Nosyk

Phys. Rev. C **91**, 014002 — Published 6 January 2015

DOI: [10.1103/PhysRevC.91.014002](https://doi.org/10.1103/PhysRevC.91.014002)

Peripheral nucleon-nucleon scattering at fifth order of chiral perturbation theory

D. R. Entem,^{1,*} N. Kaiser,^{2,†} R. Machleidt,^{3,‡} and Y. Nosyk³

¹*Grupo de Física Nuclear, IUFFyM, Universidad de Salamanca, E-37008 Salamanca, Spain*

²*Physik Department T39, Technische Universität München, D-85747 Garching, Germany*

³*Department of Physics, University of Idaho, Moscow, Idaho 83844, USA*

(Dated: November 20, 2014)

We present the two- and three-pion exchange contributions to the nucleon-nucleon interaction which occur at next-to-next-to-next-to-next-to-leading order (N⁴LO, fifth order) of chiral effective field theory, and calculate nucleon-nucleon scattering in peripheral partial waves with $L \geq 3$ using low-energy constants that were extracted from πN analysis at fourth order. While the net three-pion exchange contribution is moderate, the two-pion exchanges turn out to be sizeable and prevalingly repulsive, thus, compensating the excessive attraction characteristic for NNLO and N³LO. As a result, the N⁴LO predictions for the phase shifts of peripheral partial waves are in very good agreement with the data (with the only exception of the 1F_3 wave). We also discuss the issue of the order-by-order convergence of the chiral expansion for the NN interaction.

PACS numbers: 13.75.Cs, 21.30.-x, 12.39.Fe, 11.10.Gh

Keywords: nucleon-nucleon scattering, chiral perturbation theory, chiral effective field theory

I. INTRODUCTION

During the past three decades, it has been demonstrated that chiral effective field theory (chiral EFT) represents a powerful tool to deal with hadronic interactions at low energy in a systematic and model-independent way (see Refs. [1, 2] for recent reviews). The systematics is provided by a low-energy expansion arranged in terms of powers of the soft scale over the hard scale, $(Q/\Lambda_\chi)^\nu$, where Q is generic for an external momentum (nucleon three-momentum or pion four-momentum) or a pion mass, and $\Lambda_\chi \approx 1$ GeV the chiral symmetry breaking scale. The model-independent dynamics is created by pions interacting under the constraint of broken chiral symmetry which provides the link to low-energy QCD.

The early applications of chiral perturbation theory (ChPT) focused on systems like $\pi\pi$ [3] and πN [4], where the Goldstone-boson character of the pion guarantees that a perturbative expansion exists. But the past 20 years have also seen great progress in applying ChPT to nuclear forces [1, 2, 5–17]. About a decade ago, the nucleon-nucleon (NN) interaction up to fourth order (next-to-next-to-next-to-leading order, N³LO) was derived [7, 9, 10, 12, 13, 15] and quantitative NN potentials were developed [16, 17].

These N³LO NN potentials complemented by chiral three-nucleon forces (3NFs) have been applied in calculations of few-nucleon reactions, the structure of light- and medium-mass nuclei, and nuclear and neutron matter—with, in general, a good deal of success. However, some problems continue to exist that seem to defy any solution. The most prominent one is the so-called ‘ A_y puzzle’ of nucleon-deuteron scattering, which requires the inclusion of three-nucleon forces (3NFs) [18]. While the chiral 3NF at NNLO slightly improves the predictions for low-energy $N - d$ scattering [19], inclusion of the N³LO 3NF deteriorates the predictions [20]. Based upon general arguments, the N³LO 3NF is presumed weak, which is why one would not expect the solution of any substantial problems, anyhow. When working in the framework of an expansion, then, the obvious way to proceed is to turn to the next order, which is N⁴LO (or fifth order). Some 3NF topologies at N⁴LO have already been worked out [21, 22], and it has been shown that, at this order, all 22 possible isospin-spin-momentum 3NF structures appear. Moreover, the contributions are moderate to sizeable. What makes the fifth order even more interesting is the fact that, at this order, a new set of 3NF contact interactions appears, which has recently been derived by the Pisa group [23]. 3NF contact terms are attractive from the point of view of the practitioner, because they are typically simple (as compared to loop contributions) and their coefficients are essentially free. Thus, at N⁴LO, the A_y puzzle may be solved in a trivial way through 3NF (contact) interactions. Due to the great diversity of structures offered at N⁴LO, one can also expect that other persistent nuclear structure problems may finally find their solution at N⁴LO.

*Electronic address: entem@usal.es

†Electronic address: nkaiser@ph.tum.de

‡Electronic address: machleidt@uidaho.edu

A principle of all EFTs is that, for reliable predictions, it is necessary that all terms included are evaluated at the order at which the calculation is conducted. Thus, if nuclear structure problems require for their solution the inclusion of 3NFs at N⁴LO, then also the two-nucleon force involved in the calculation has to be of order N⁴LO. This is one reason for the investigation of the NN interaction at N⁴LO presented in this paper. Besides this, there are also some more specific issues that motivate a study of this kind. From calculations of the NN interaction at NNLO [7] and N³LO [15], it is wellknown that there is a problem with excessive attraction, particularly, when for the c_i low-energy constants (LECs) of the dimension-two πN Lagrangian the values are applied that are obtained from πN analysis. It is important to know if this problem is finally solved when going beyond N³LO. Last not least, also the convergence of the chiral expansion of the NN interaction is of general interest.

This paper is organized as follows: In Sec. II, we derive the two- and three-pion exchange contributions at fifth order. The predictions for NN scattering in peripheral partial waves are shown in Sec. III, and Sec. IV concludes the paper. In the Appendices, we summarize the detailed mathematical expressions that define the lower orders of the chiral NN potential. This is necessary, because in this study we perform the power counting (of relativistic $1/M_N$ -corrections) differently as compared to our earlier work. Since we present also phase shift predictions for the lower orders, the unambiguous definition of each order is necessary to avoid confusion.

II. PION-EXCHANGE CONTRIBUTIONS TO THE NN POTENTIAL

The various pion-exchange contributions to the NN potential may be analyzed according to the number of pions being exchanged between the two nucleons:

$$V = V_{1\pi} + V_{2\pi} + V_{3\pi} + \dots, \quad (2.1)$$

where the meaning of the subscripts is obvious and the ellipsis represents 4π and higher pion exchanges. For each of the above terms, we have a low-momentum expansion:

$$V_{1\pi} = V_{1\pi}^{(0)} + V_{1\pi}^{(2)} + V_{1\pi}^{(3)} + V_{1\pi}^{(4)} + V_{1\pi}^{(5)} + \dots \quad (2.2)$$

$$V_{2\pi} = V_{2\pi}^{(2)} + V_{2\pi}^{(3)} + V_{2\pi}^{(4)} + V_{2\pi}^{(5)} + \dots \quad (2.3)$$

$$V_{3\pi} = V_{3\pi}^{(4)} + V_{3\pi}^{(5)} + \dots, \quad (2.4)$$

where the superscript denotes the order ν of the expansion, which for an irreducible two-nucleon diagram is given by $\nu = 2L + \sum_i (d_i + n_i/2 - 2)$ with L the number of loops, d_i is the number of derivatives or pion-mass insertions, and n_i the number of nucleon fields (nucleon legs) involved in vertex i . The sum runs over all vertices contained in the diagram under consideration.

Order by order, the NN potential builds up as follows:

$$V_{\text{LO}} \equiv V^{(0)} = V_{1\pi}^{(0)} \quad (2.5)$$

$$V_{\text{NLO}} \equiv V^{(2)} = V_{\text{LO}} + V_{1\pi}^{(2)} + V_{2\pi}^{(2)} \quad (2.6)$$

$$V_{\text{NNLO}} \equiv V^{(3)} = V_{\text{NLO}} + V_{1\pi}^{(3)} + V_{2\pi}^{(3)} \quad (2.7)$$

$$V_{\text{N3LO}} \equiv V^{(4)} = V_{\text{NNLO}} + V_{1\pi}^{(4)} + V_{2\pi}^{(4)} + V_{3\pi}^{(4)} \quad (2.8)$$

$$V_{\text{N4LO}} \equiv V^{(5)} = V_{\text{N3LO}} + V_{1\pi}^{(5)} + V_{2\pi}^{(5)} + V_{3\pi}^{(5)} \quad (2.9)$$

where LO stands for leading order, NLO for next-to-leading order, etc..

In past work [6–10, 12–17], the NN interaction has been developed up to N³LO. To make this paper selfcontained and, because we perform the power counting for relativistic corrections differently as compared to our previous work, we summarize, order by order, the contributions up to N³LO in the Appendices. In this way, all orders, which we are talking about in this paper, are unambiguously defined.

The novel feature of this paper are the contributions to the NN potential at N⁴LO, which we will present now.

The results will be stated in terms of contributions to the momentum-space NN amplitudes in the center-of-mass system (CMS), which arise from the following general decomposition:

$$\begin{aligned} V(\vec{p}', \vec{p}) = & V_C + \boldsymbol{\tau}_1 \cdot \boldsymbol{\tau}_2 W_C \\ & + [V_S + \boldsymbol{\tau}_1 \cdot \boldsymbol{\tau}_2 W_S] \vec{\sigma}_1 \cdot \vec{\sigma}_2 \\ & + [V_{LS} + \boldsymbol{\tau}_1 \cdot \boldsymbol{\tau}_2 W_{LS}] \left(-i\vec{S} \cdot (\vec{q} \times \vec{k}) \right) \\ & + [V_T + \boldsymbol{\tau}_1 \cdot \boldsymbol{\tau}_2 W_T] \vec{\sigma}_1 \cdot \vec{q} \vec{\sigma}_2 \cdot \vec{q} \\ & + [V_{\sigma L} + \boldsymbol{\tau}_1 \cdot \boldsymbol{\tau}_2 W_{\sigma L}] \vec{\sigma}_1 \cdot (\vec{q} \times \vec{k}) \vec{\sigma}_2 \cdot (\vec{q} \times \vec{k}), \end{aligned} \quad (2.10)$$

where \vec{p}' and \vec{p} denote the final and initial nucleon momenta in the CMS, respectively. Moreover, $\vec{q} = \vec{p}' - \vec{p}$ is the momentum transfer, $\vec{k} = (\vec{p}' + \vec{p})/2$ the average momentum, and $\vec{S} = (\vec{\sigma}_1 + \vec{\sigma}_2)/2$ the total spin, with $\vec{\sigma}_{1,2}$ and $\tau_{1,2}$ the spin and isospin operators, of nucleon 1 and 2, respectively. For on-shell scattering, V_α and W_α ($\alpha = C, S, LS, T, \sigma L$) can be expressed as functions of $q = |\vec{q}|$ and $p = |\vec{p}'| = |\vec{p}|$, only. Note that the one-pion exchange contribution in Eq. (2.2) is of the form $W_T^{(1\pi)} = -(g_{\pi N}/2M_N)^2(m_\pi^2 + q^2)^{-1}$ with physical values of the coupling constant $g_{\pi N}$ and nucleon and pion masses M_N and m_π . This expression fixes at the same time our sign-convention for $V(\vec{p}', \vec{p})$.

We will state two-loop contributions in terms of their spectral functions, from which the momentum-space amplitudes $V_\alpha(q)$ and $W_\alpha(q)$ are obtained via the subtracted dispersion integrals:

$$\begin{aligned} V_{C,S}(q) &= -\frac{2q^6}{\pi} \int_{nm_\pi}^{\tilde{\Lambda}} d\mu \frac{\text{Im} V_{C,S}(i\mu)}{\mu^5(\mu^2 + q^2)}, \\ V_T(q) &= \frac{2q^4}{\pi} \int_{nm_\pi}^{\tilde{\Lambda}} d\mu \frac{\text{Im} V_T(i\mu)}{\mu^3(\mu^2 + q^2)}, \end{aligned} \quad (2.11)$$

and similarly for $W_{C,S,T}$. Clearly, $n = 2$ for two-pion exchange and $n = 3$ for three-pion exchange. For $\tilde{\Lambda} \rightarrow \infty$ the above dispersion integrals yield the results of dimensional regularization, while for finite $\tilde{\Lambda} \gtrsim nm_\pi$ we have what has become known as spectral-function regularization (SFR) [27]. The purpose of the finite scale $\tilde{\Lambda}$ is to constrain the imaginary parts to the low-momentum region where chiral effective field theory is applicable.

A. Two-pion exchange contributions at N⁴LO

The 2π -exchange contributions that occur at N⁴LO are displayed graphically in Fig. 1. We present now the corresponding analytical expressions separately for each class.

1. Spectral functions for class (a)

The N⁴LO 2π -exchange two-loop contributions of class (a) are shown in Fig. 1(a). For this class the spectral functions are obtained by integrating the product of the leading one-loop πN amplitude and the chiral $\pi\pi NN$ vertex proportional to c_i over the Lorentz-invariant 2π -phase space. In the $\pi\pi$ center-of-mass frame this integral can be expressed as an angular integral $\int_{-1}^1 dx$ [12]. The results for the non-vanishing spectral functions read:

$$\begin{aligned} \text{Im}V_C &= -\frac{m_\pi^5}{(4f_\pi)^6\pi^2} \left\{ g_A^2 \sqrt{u^2 - 4} \left(5 - 2u^2 - \frac{2}{u^2} \right) \left[24c_1 + c_2(u^2 - 4) + 6c_3(u^2 - 2) \right] \ln \frac{u+2}{u-2} \right. \\ &\quad + \frac{8}{u} \left[3(4c_1 + c_3(u^2 - 2))(4g_A^4 u^2 - 10g_A^4 + 1) + c_2(6g_A^4 u^2 - 10g_A^4 - 3) \right] B(u) \\ &\quad + \sqrt{u^2 - 4} \left[3(2 - u^2)(4c_1 + c_3(u^2 - 2)) + c_2(7u^2 - 6 - u^4) + \frac{4g_A^2}{u}(2u^2 - 1) \right. \\ &\quad \times \left[4(6c_1 - c_2 - 3c_3) + (c_2 + 6c_3)u^2 \right] + 4g_A^4 \left(\frac{32}{u+2}(2c_1 + c_3) + \frac{64}{3u}(6c_1 + c_2 - 3c_3) \right. \\ &\quad \left. \left. \left. + 14c_3 - 5c_2 - 92c_1 + \frac{8u}{3}(18c_3 - 5c_2) + \frac{u^2}{6}(36c_1 + 13c_2 - 156c_3) + \frac{u^4}{6}(2c_2 + 9c_3) \right) \right] \right\}, \end{aligned} \quad (2.12)$$

$$\begin{aligned} \text{Im}W_S &= \mu^2 \text{Im}W_T = \frac{c_4 g_A^2 m_\pi^5}{(4f_\pi)^6\pi^2} \left\{ 8g_A^2 u(5 - u^2)B(u) + \frac{1}{3}(u^2 - 4)^{5/2} \ln \frac{u+2}{u-2} \right. \\ &\quad \left. + \frac{u}{3} \sqrt{u^2 - 4} \left[g_A^2(30u - u^3 - 64) - 4u^2 + 16 \right] \right\}, \end{aligned} \quad (2.13)$$

with the dimensionless variable $u = \mu/m_\pi > 2$ and the logarithmic function

$$B(u) = \ln \frac{u + \sqrt{u^2 - 4}}{2}. \quad (2.14)$$

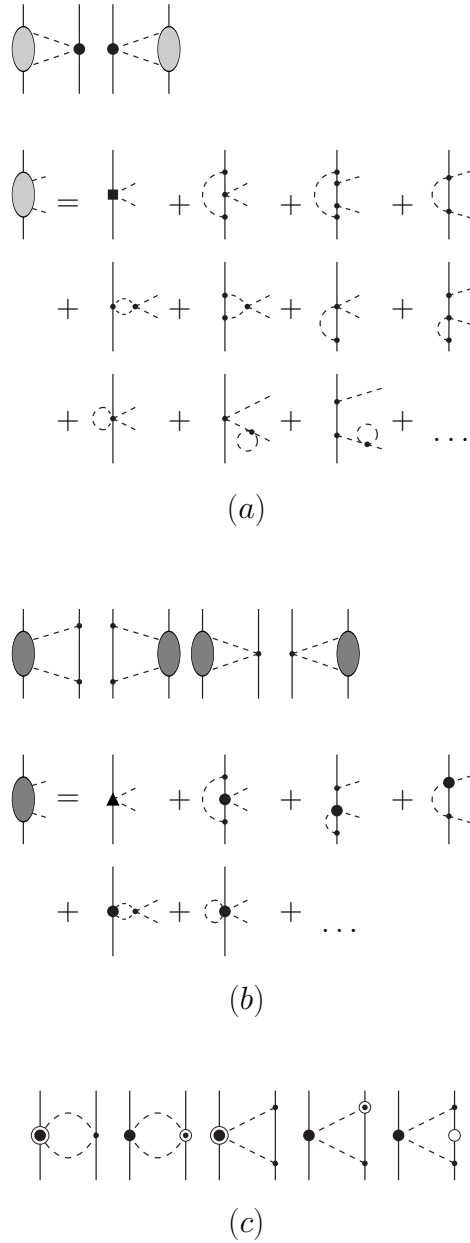


FIG. 1: Two-pion-exchange contributions at N⁴LO. (a) The leading one-loop πN amplitude is folded with the chiral $\pi\pi NN$ vertices proportional to c_i . (b) The one-loop πN amplitude proportional to c_i is folded with the leading order chiral πN amplitude. (c) Relativistic corrections of NNLO diagrams. Solid lines represent nucleons and dashed lines pions. Small dots, large solid dots, solid squares, and triangles denote vertices of index $d_i + n_i/2 - 2 = 0, 1, 2,$ and $3,$ respectively. Open circles are relativistic $1/M_N$ corrections.

2. Spectral functions for class (b)

The N⁴LO 2π -exchange two-loop contributions of class (b) are displayed in Fig. 1(b). For this class, the product of the one-loop πN amplitude proportional to c_i (see Ref. [21] for details) and the leading order chiral πN amplitude

is integrated over the 2π -phase space. We obtain:

$$\text{Im}V_S = \mu^2 \text{Im}V_T = \frac{g_A^4 m_\pi^5 (c_3 - c_4) u}{(4f_\pi)^6 \pi^2} \left\{ \sqrt{u^2 - 4} (u^3 - 30u + 64) + 24(u^2 - 5)B(u) \right\}, \quad (2.15)$$

$$\begin{aligned} \text{Im}W_S = \mu^2 \text{Im}W_T = & \frac{g_A^2 m_\pi^5}{(4f_\pi)^6 \pi^2} (4 - u^2) \left\{ \frac{c_4}{3} \left[\sqrt{u^2 - 4} (2u^2 - 8)B(u) \right. \right. \\ & \left. \left. + 4u(2 + 9g_A^2) - \frac{5u^3}{3} \right] + 2\bar{e}_{17}(8\pi f_\pi)^2 (u^3 - 2u) \right\}, \end{aligned} \quad (2.16)$$

$$\begin{aligned} \text{Im}V_C = & \frac{g_A^2 m_\pi^5}{(4f_\pi)^6 \pi^2} (u^2 - 2) \left(\frac{1}{u^2} - 2 \right) \left\{ 2\sqrt{u^2 - 4} \left[24c_1 + c_2(u^2 - 4) + 6c_3(u^2 - 2) \right] B(u) \right. \\ & \left. + u \left[c_2 \left(8 - \frac{5u^2}{3} \right) + 6c_3(2 - u^2) - 24c_1 \right] \right\} + \frac{3g_A^2 m_\pi^5}{(2f_\pi)^4 u} (2 - u^2)^3 \bar{e}_{14}, \end{aligned} \quad (2.17)$$

$$\begin{aligned} \text{Im}W_C = & -\frac{c_1 m_\pi^5}{(2f_\pi)^6 \pi^2} \left\{ \frac{3g_A^2 + 1}{8} \sqrt{u^2 - 4} (2 - u^2) + \left(\frac{3g_A^2 + 1}{u} - 2g_A^2 u \right) B(u) \right\} \\ & -\frac{c_2 m_\pi^5}{(2f_\pi)^6 \pi^2} \left\{ \frac{1}{96} \sqrt{u^2 - 4} \left[7u^2 - 6 - u^4 + g_A^2 (5u^2 - 6 - 2u^4) \right] + \frac{1}{4u} (g_A^2 u^2 - 1 - g_A^2) B(u) \right\} \\ & -\frac{c_3 m_\pi^5}{(4f_\pi)^6 \pi^2} \left\{ \frac{2}{9} \sqrt{u^2 - 4} \left[3(7u^2 - 6 - u^4) + 4g_A^2 \left(\frac{32}{u} - 12 - 20u + 7u^2 - u^4 \right) \right. \right. \\ & \left. \left. + g_A^4 \left(114 - \frac{512}{u} + 368u - 169u^2 + 7u^4 + \frac{192}{u+2} \right) \right] \right. \\ & \left. + \frac{16}{3u} \left[g_A^4 (6u^4 - 30u^2 + 35) + g_A^2 (6u^2 - 8) - 3 \right] B(u) \right\} \\ & -\frac{c_4 g_A^2 m_\pi^5}{(4f_\pi)^6 \pi^2} \left\{ \frac{2}{9} \sqrt{u^2 - 4} \left[30 - \frac{128}{u} + 80u - 13u^2 - 2u^4 + g_A^2 \left(\frac{512}{u} - 114 - 368u \right. \right. \right. \\ & \left. \left. \left. + 169u^2 - 7u^4 - \frac{192}{u+2} \right) \right] + \frac{16}{3u} \left[5 - 3u^2 + g_A^2 (30u^2 - 35 - 6u^4) \right] B(u) \right\}. \end{aligned} \quad (2.18)$$

Consistent with the calculation of the πN amplitude in Ref. [21], we applied relations between LECs, such that only \bar{e}_{14} and \bar{e}_{17} remain in the final result.

3. Relativistic corrections

This group consists of diagrams with one vertex proportional to c_i and one $1/M_N$ correction. A few representative graphs are shown in Fig. 1(c). Since in this investigation we count $Q/M_N \sim (Q/\Lambda_\chi)^2$, these relativistic corrections are formally of order $N^4\text{LO}$. The result for this group of diagrams read in our sign-convention [12]:

$$V_C = \frac{g_A^2 L(\tilde{\Lambda}; q)}{32\pi^2 M_N f_\pi^4} \left[(6c_3 - c_2)q^4 + 4(3c_3 - c_2 - 6c_1)q^2 m_\pi^2 + 6(2c_3 - c_2)m_\pi^4 - 24(2c_1 + c_3)m_\pi^6 w^{-2} \right], \quad (2.19)$$

$$W_C = -\frac{c_4}{192\pi^2 M_N f_\pi^4} \left[g_A^2 (8m_\pi^2 + 5q^2) + w^2 \right] q^2 L(\tilde{\Lambda}; q), \quad (2.20)$$

$$W_T = -\frac{1}{q^2} W_S = \frac{c_4}{192\pi^2 M_N f_\pi^4} \left[w^2 - g_A^2 (16m_\pi^2 + 7q^2) \right] L(\tilde{\Lambda}; q), \quad (2.21)$$

$$V_{LS} = \frac{c_2 g_A^2}{8\pi^2 M_N f_\pi^4} w^2 L(\tilde{\Lambda}; q), \quad (2.22)$$

$$W_{LS} = -\frac{c_4}{48\pi^2 M_N f_\pi^4} \left[g_A^2 (8m_\pi^2 + 5q^2) + w^2 \right] L(\tilde{\Lambda}; q), \quad (2.23)$$

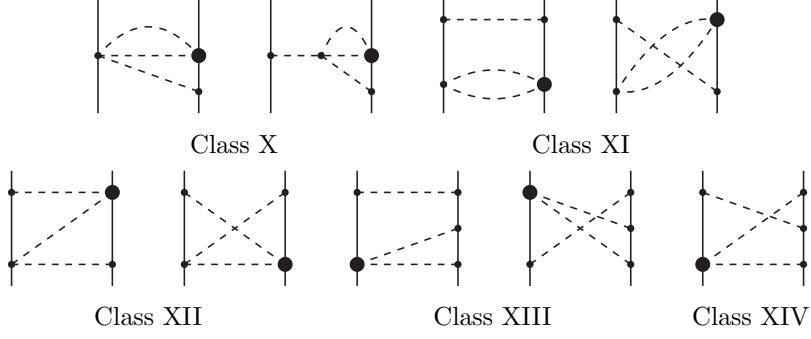


FIG. 2: Three-pion exchange contributions at $N^4\text{LO}$. The classification scheme of Ref. [11] is used. Notation as in Fig. 1.

where the (regularized) logarithmic loop function is given by:

$$L(\tilde{\Lambda}; q) = \frac{w}{2q} \ln \frac{\tilde{\Lambda}^2(2m_\pi^2 + q^2) - 2m_\pi^2 q^2 + \tilde{\Lambda} \sqrt{\tilde{\Lambda}^2 - 4m_\pi^2} q w}{2m_\pi^2(\tilde{\Lambda}^2 + q^2)} \quad (2.24)$$

with $w = \sqrt{4m_\pi^2 + q^2}$. Note that

$$\lim_{\tilde{\Lambda} \rightarrow \infty} L(\tilde{\Lambda}; q) = \frac{w}{q} \ln \frac{w + q}{2m_\pi}, \quad (2.25)$$

is the logarithmic loop function of dimensional regularization.

B. Three-pion exchange contributions at $N^4\text{LO}$

The 3π -exchange of order $N^4\text{LO}$ is shown in Fig. 2. The spectral functions for these diagrams have been calculated in Ref. [11]. We use here the classification scheme introduced in that reference and note that class XI vanishes. Moreover, we find that the class X and part of class XIV make only negligible contributions. Thus, we include in our calculations only class XII and XIII, and the V_S contribution of class XIV. In Ref. [11] the spectral functions were presented in terms of an integral over the invariant mass of a pion pair. We have solved these integrals analytically and obtain the following spectral functions for the non-negligible cases:

$$\begin{aligned} \text{Im } V_S^{(\text{XII})} &= -\frac{g_A^2 c_4 m_\pi^5}{(4f_\pi)^6 \pi^2 u^3} \left[\frac{y}{12} (u-1)(100u^3 - 27 - 50u - 151u^2 + 185u^4 - 14u^5 - 7u^6) \right. \\ &\quad \left. + 4D(u)(2 + 10u^2 - 9u^4) \right], \end{aligned} \quad (2.26)$$

$$\begin{aligned} \text{Im } V_T^{(\text{XII})} &= \frac{1}{\mu^2} \text{Im } V_S^{(\text{XII})} - \frac{g_A^2 c_4 m_\pi^3}{(4f_\pi)^6 \pi^2 u^5} \left[\frac{y}{6} (u-1)(u^6 + 2u^5 - 39u^4 - 12u^3 + 65u^2 - 50u - 27) \right. \\ &\quad \left. + 8D(u)(3u^4 - 10u^2 + 2) \right], \end{aligned} \quad (2.27)$$

$$\begin{aligned} \text{Im } W_S^{(\text{XII})} &= -\frac{g_A^2 m_\pi^5}{(4f_\pi)^6 \pi^2 u^3} \left\{ y(u-1) \left[\frac{4c_1 u}{3} (u^3 + 2u^2 - u + 4) + \frac{c_2}{72} (u^6 + 2u^5 - 39u^4 - 12u^3 + 65u^2 - 50u - 27) \right. \right. \\ &\quad \left. \left. + \frac{c_3}{12} (u^6 + 2u^5 - 31u^4 + 4u^3 + 57u^2 - 18u - 27) \right. \right. \\ &\quad \left. \left. + \frac{c_4}{72} (7u^6 + 14u^5 - 185u^4 - 100u^3 + 151u^2 + 50u + 27) \right] \right. \\ &\quad \left. + D(u) \left[16c_1(4u^2 - 1 - u^4) + \frac{2c_2}{3} (2 - 10u^2 + 3u^4) + 4c_3 u^2 (u^2 - 2) + \frac{2c_4}{3} (9u^4 - 10u^2 - 2) \right] \right\} \quad (2.28) \end{aligned}$$

$$\begin{aligned}
\text{Im } W_T^{(\text{XII})} = & \frac{1}{\mu^2} \text{Im } W_S^{(\text{XII})} - \frac{g_A^2 m_\pi^3}{(4f_\pi)^6 \pi^2 u^5} \left\{ y(u-1) \left[\frac{16c_1 u}{3} (2+u-2u^2-u^3) \right. \right. \\
& + \frac{c_2}{36} (73u^4 - 6u^5 - 3u^6 + 44u^3 - 43u^2 - 50u - 27) \\
& + \frac{c_3}{2} (19u^4 - 2u^5 - u^6 + 4u^3 - 9u^2 - 6u - 9) \\
& \left. \left. + \frac{c_4}{36} (39u^4 - 2u^5 - u^6 + 12u^3 - 65u^2 + 50u + 27) \right] \right. \\
& \left. + 4D(u) \left[8c_1(u^4 - 1) + c_2 \left(\frac{2}{3} - u^4 \right) - 2c_3 u^4 + \frac{c_4}{3} (10u^2 - 2 - 3u^4) \right] \right\}, \quad (2.29)
\end{aligned}$$

$$\text{Im } W_C^{(\text{XIII})} = -\frac{g_A^4 c_4 m_\pi^5}{(4f_\pi)^6 \pi^2} \left[\frac{8y}{3} (u-1)(u-4-2u^2-u^3) + 32D(u) \left(u^3 - 4u + \frac{1}{u} \right) \right], \quad (2.30)$$

$$\begin{aligned}
\text{Im } V_S^{(\text{XIII})} = & -\frac{g_A^4 c_4 m_\pi^5}{(4f_\pi)^6 \pi^2 u^3} \left[\frac{y}{24} (u-1)(37u^6 + 74u^5 - 251u^4 - 268u^3 + 349u^2 - 58u - 135) \right. \\
& \left. + 2D(u) (39u^4 - 2 - 52u^2 - 6u^6) \right], \quad (2.31)
\end{aligned}$$

$$\begin{aligned}
\text{Im } V_T^{(\text{XIII})} = & \frac{1}{\mu^2} \text{Im } V_S^{(\text{XIII})} - \frac{g_A^4 c_4 m_\pi^3}{(4f_\pi)^6 \pi^2 u^5} \left[\frac{y}{12} (u-1)(5u^6 + 10u^5 - 3u^4 - 252u^3 - 443u^2 - 58u - 135) \right. \\
& \left. + 4D(u) (3u^4 + 22u^2 - 2) \right], \quad (2.32)
\end{aligned}$$

$$\begin{aligned}
\text{Im } W_S^{(\text{XIII})} = & -\frac{g_A^4 m_\pi^5}{(4f_\pi)^6 \pi^2 u^3} \left\{ y(u-1) \left[2c_1 u (5u^3 + 10u^2 - 5u - 4) \right. \right. \\
& + \frac{c_2}{48} (135 + 58u - 277u^2 - 36u^3 + 147u^4 - 10u^5 - 5u^6) \\
& + \frac{c_3}{8} (7u^6 + 14u^5 - 145u^4 - 20u^3 + 111u^2 + 18u + 27) \\
& \left. \left. + \frac{c_4}{6} (44u^3 + 37u^4 - 14u^5 - 7u^6 - 3u^2 - 18u - 27) \right] \right. \\
& \left. + D(u) \left[24c_1(1 + 4u^2 - 3u^4) + c_2(2 + 2u^2 - 3u^4) + 6c_3 u^2(3u^2 - 2) + 8c_4 u^2(u^4 - 5u^2 + 5) \right] \right\}, \quad (2.33)
\end{aligned}$$

$$\begin{aligned}
\text{Im } W_T^{(\text{XIII})} = & \frac{1}{\mu^2} \text{Im } W_S^{(\text{XIII})} - \frac{g_A^4 m_\pi^3}{(4f_\pi)^6 \pi^2 u^5} \left\{ y(u-1) \left[4c_1 u (5u^3 + 10u^2 + 7u - 4) \right. \right. \\
& + \frac{c_2}{24} (135 + 58u + 227u^2 + 204u^3 + 27u^4 - 10u^5 - 5u^6) \\
& + \frac{c_3}{4} (27 + 18u - 9u^2 - 68u^3 - 121u^4 + 14u^5 + 7u^6) \\
& \left. \left. + c_4(4u^3 + 19u^4 - 2u^5 - u^6 - 9u^2 - 6u - 9) \right] \right. \\
& \left. + 2D(u) \left[24c_1(1 - 3u^4) + c_2(2 - 10u^2 - 3u^4) + 6c_3 u^2(3u^2 + 2) - 8c_4 u^4 \right] \right\}, \quad (2.34)
\end{aligned}$$

$$\begin{aligned}
\text{Im } V_S^{(\text{XIV})} = & -\frac{g_A^4 c_4 m_\pi^5}{(4f_\pi)^6 \pi^2 u^3} \left[\frac{y}{24} (u-1)(637u^2 - 58u - 135 + 116u^3 - 491u^4 - 22u^5 - 11u^6) \right. \\
& \left. + 2D(u) (6u^6 - 9u^4 + 8u^2 - 2) \right], \quad (2.35)
\end{aligned}$$

where $y = \sqrt{(u-3)(u+1)}$ and $D(u) = \ln[(u-1+y)/2]$ with $u = \mu/m_\pi > 3$.

III. PERTURBATIVE NN SCATTERING IN PERIPHERAL PARTIAL WAVES

Nucleon-nucleon scattering in peripheral partial waves is of special interest—for several reasons. First, these partial waves probe the long- and intermediate-range of the nuclear force. Due to the centrifugal barrier, there is only small sensitivity to short-range contributions and, in fact, the contact terms up to and including order $N^3\text{LO}$ make no contributions for orbital angular momenta $L \geq 3$. Thus, for F and higher waves and energies below the pion-production threshold, we have a window in which the NN interaction is governed by chiral symmetry alone (chiral one- and multi-pion exchanges), and we can conduct a relatively clean test of how well the theory works. Using values for the LECs from πN analysis, the NN predictions are even parameter free. Moreover, the smallness of the phase shifts in peripheral partial waves suggests that the calculation can be done perturbatively. This avoids the complications and possible model-dependence (e.g., cutoff dependence) that the non-perturbative treatment of the Lippmann-Schwinger equation, necessary for low partial waves, is beset with. A thorough investigation of this kind at $N^3\text{LO}$ was conducted in Ref. [15]. Here, we will work at $N^4\text{LO}$.

The perturbative K -matrix for np scattering is calculated as follows:

$$K(\vec{p}', \vec{p}) = V_{1\pi}^{(np)}(\vec{p}', \vec{p}) + V_{2\pi, \text{it}}^{(np)}(\vec{p}', \vec{p}) + V(\vec{p}', \vec{p}) \quad (3.1)$$

with $V_{1\pi}^{(np)}(\vec{p}', \vec{p})$ as in Eq. (A2), and $V_{2\pi, \text{it}}^{(np)}(\vec{p}', \vec{p})$ representing the once iterated one-pion exchange (1PE) given by

$$V_{2\pi, \text{it}}^{(np)}(\vec{p}', \vec{p}) = \mathcal{P} \int d^3 p'' \frac{M_N^2}{E_{p''}} \frac{V_{1\pi}^{(np)}(\vec{p}', \vec{p}'') V_{1\pi}^{(np)}(\vec{p}'', \vec{p})}{p^2 - p''^2}, \quad (3.2)$$

where \mathcal{P} denotes the principal value integral and $E_{p''} = \sqrt{M_N^2 + p''^2}$. A calculation at LO includes only the first term on the right hand side of Eq. (3.1), $V_{1\pi}^{(np)}(\vec{p}', \vec{p})$, while calculations at NLO or higher order also include the second term on the right hand side, $V_{2\pi, \text{it}}^{(np)}(\vec{p}', \vec{p})$. At $N^3\text{LO}$ and beyond, the twice iterated 1PE should be included, too. However, we found that the difference between the once iterated 1PE and the infinitely iterated 1PE is so small that it could not be identified on the scale of our phase shift figures. For that reason, we omit iterations of 1PE beyond what is contained in $V_{2\pi, \text{it}}^{(np)}(\vec{p}', \vec{p})$.

Finally, the third term on the r.h.s. of Eq. (3.1), $V(\vec{p}', \vec{p})$, stands for the irreducible multi-pion exchange contributions that occur at the order at which the calculation is conducted. In multi-pion exchanges, we use the average pion mass $m_\pi = 138.039$ MeV and, thus, neglect the charge-dependence due to pion-mass splitting in irreducible multi-pion diagrams. The charge-dependence that emerges from irreducible 2π exchange was investigated in Ref. [28] and found to be negligible for partial waves with $L \geq 3$.

Throughout this paper, we use

$$M_N = \frac{2M_p M_n}{M_p + M_n} = 938.9182 \text{ MeV}. \quad (3.3)$$

Based upon relativistic kinematics, the CMS on-shell momentum p is related to the kinetic energy of the incident neutron in the laboratory system (“Lab. Energy”), T_{lab} , by

$$p^2 = \frac{M_p^2 T_{\text{lab}} (T_{\text{lab}} + 2M_n)}{(M_p + M_n)^2 + 2T_{\text{lab}} M_p}, \quad (3.4)$$

with $M_p = 938.2720$ MeV and $M_n = 939.5653$ MeV the proton and neutron masses, respectively.

The K -matrix, Eq. (3.1), is decomposed into partial waves following Ref. [29] and phase shifts are then calculated via

$$\tan \delta_L(T_{\text{lab}}) = -\frac{M_N^2 p}{16\pi^2 E_p} p K_L(p, p). \quad (3.5)$$

For more details concerning the evaluation of phase shifts, including the case of coupled partial waves, see Ref. [30] or the appendix of [31]. All phase shifts shown in this paper are in terms of Stapp conventions [32].

We calculate phase shifts for partial waves with $L \geq 3$ and $T_{\text{lab}} \leq 300$ MeV. To establish a link between πN and NN and to check the consistency of the πN and NN systems, we use the πN LECs determined in Ref. [21] in a calculation of πN scattering at fourth order applying the same power counting scheme as in the present work. To be specific, we use the set of LECs denoted by ‘KH’ in Ref. [21]. The values are:

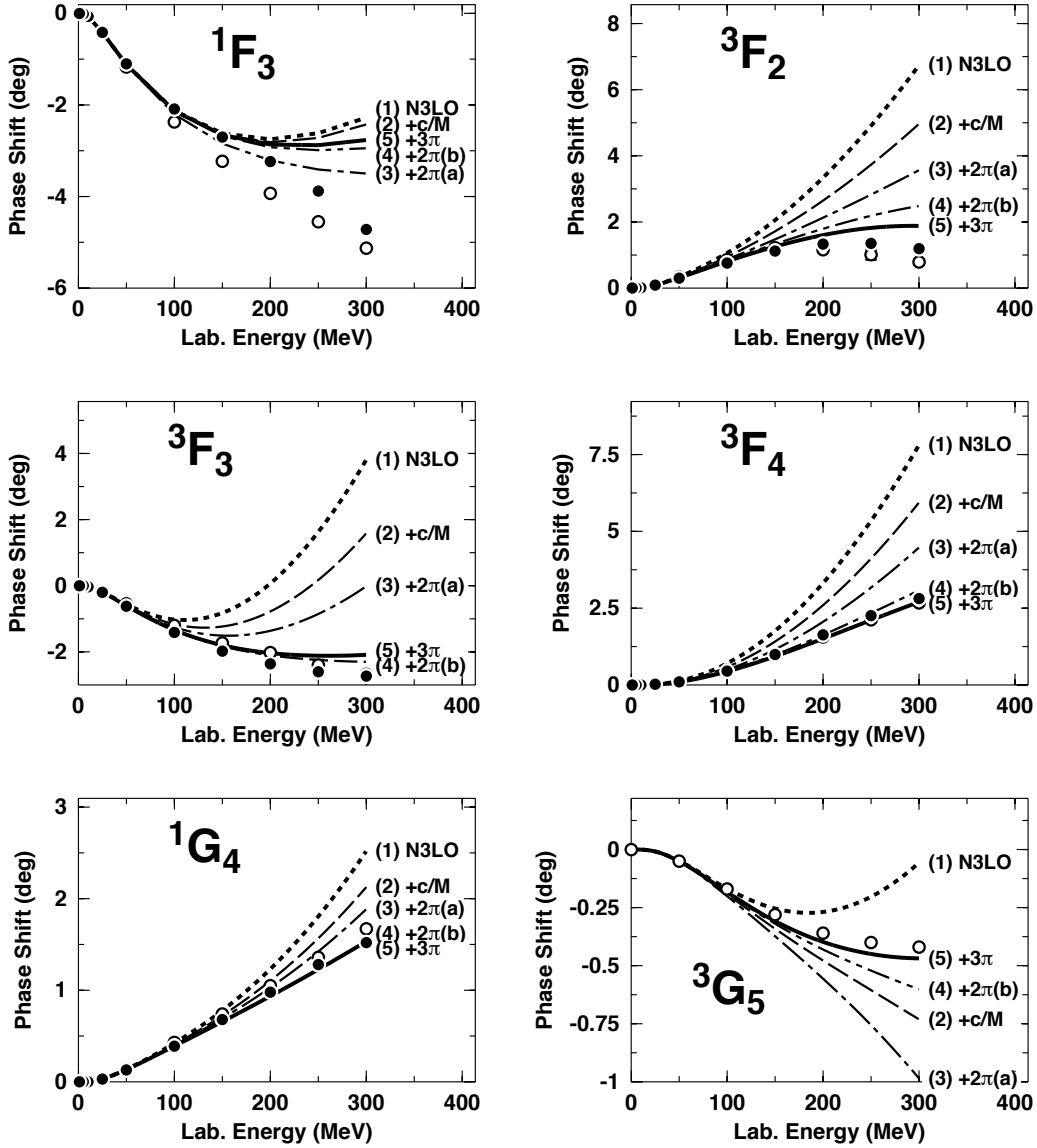


FIG. 3: Effect of individual fifth-order contributions on the neutron-proton phase shifts of some selected peripheral partial waves. The individual contributions are added up successively in the order given in parenthesis next to each curve. Curve (1) is N3LO and curve (5) is the complete N4LO. The filled and open circles represent the results from the Nijmegen multi-energy np phase-shift analysis [33] and the VPI/GWU single-energy np analysis SM99 [34], respectively.

$$c_1 = -0.75 \text{ GeV}^{-1}, \quad c_2 = 3.49 \text{ GeV}^{-1}, \quad c_3 = -4.77 \text{ GeV}^{-1}, \quad c_4 = 3.34 \text{ GeV}^{-1};$$

$$\bar{d}_1 + \bar{d}_2 = 6.21 \text{ GeV}^{-2}, \quad \bar{d}_3 = -6.83 \text{ GeV}^{-2}, \quad \bar{d}_5 = 0.78 \text{ GeV}^{-2}, \quad \bar{d}_{14} - \bar{d}_{15} = -12.02 \text{ GeV}^{-2};$$

$$\bar{e}_{14} = 1.52 \text{ GeV}^{-3}, \quad \bar{e}_{17} = -0.37 \text{ GeV}^{-3}.$$

Moreover, we absorb the Goldberger-Treiman discrepancy into an effective value for g_A , namely, $g_A = 1.29$.

Finally, the physical value of the pion-decay constant is $f_\pi = 92.4$ MeV.

As shown in Figs. 1 and 2 and derived in Sec. II, the fifth order consists of several contributions. We will now demonstrate how the individual fifth-order contributions impact NN phase shifts in peripheral waves. For this purpose, we display in Fig. 3 phase shifts for six important peripheral partial waves, namely, 1F_3 , 3F_2 , 3F_3 , 3F_4 , 1G_4 , and 3G_5 . In each frame, the following curves are shown:

- (1) N³LO.
- (2) The previous curve plus the c_i/M_N corrections (denoted by ‘c/M’), Fig. 1(c) and Sec. II A 3.
- (3) The previous curve plus the N⁴LO 2 π -exchange (2PE) two-loop contributions of class (a), Fig. 1(a) and Sec. II A 1.
- (4) The previous curve plus the N⁴LO 2PE two-loop contributions of class (b), Fig. 1(b) and Sec. II A 2.
- (5) The previous curve plus the N⁴LO 3 π -exchange (3PE) contributions, Fig. 2 and Sec. II B.

In summary, the various curves add up successively the individual N⁴LO contributions in the order indicated in the curve labels. The last curve in this series, curve (5), is the full N⁴LO result. In these calculations, a SFR cutoff $\tilde{\Lambda} = 1.5$ GeV is applied [cf. Eq. (2.11)].

From Fig. 3, we make the following observations. In triplet F -waves, the c_i/M_N corrections as well as the 2PE two-loops, class (a) and (b), are all repulsive and of about the same strength. As a consequence, the problem of the excessive attraction, that N³LO is beset with, is overcome. A similar trend is seen in 1G_4 . An exception is 1F_3 , where the class (b) contribution is attractive leading to phase shifts above the data for energies higher than 150 MeV.

Now turning to the N⁴LO 3PE contributions [curve (5) in Fig. 3]: they are substantially smaller than the 2PE two-loop ones, in all peripheral partial waves. This can be interpreted as an indication of convergence with regard to the number of pions being exchanged between two nucleons—a trend that is very welcome. Further, note that the total 3PE contribution is a very comprehensive one, cf. Fig. 2. It is the sum of ten terms (cf. Sec. II B) which, individually, can be fairly large. However, destructive interference between them leads to the small net result.

For all F and G waves (except 1F_3), the final N⁴LO result is in excellent agreement with the empirical phase shifts. Notice that this includes also 3G_5 , which posed persistent problems at N³LO [15].

On a historical note, we mention that in the construction of the Stony Brook [35, 36] and Paris [37, 38] NN potentials, which both include a 2PE contribution based upon dispersion theory, the dispersion integral, Eq. (2.11), is cutoff at $\mu^2 = 50 m_\pi^2$, which is equivalent to a SFR cutoff $\tilde{\Lambda} = \sqrt{50} m_\pi \sim 1$ GeV. Not accidentally, this agrees well with the common assumption of $\Lambda_\chi \sim 1$ GeV and, thus, sets the scale for an appropriate choice of $\tilde{\Lambda}$. Consistent with this, $\tilde{\Lambda} = 1.5$ GeV was used for the results presented in Fig. 3. It is, however, also of interest to know how predictions change with variations of $\tilde{\Lambda}$ within a reasonable range. We have, therefore, varied $\tilde{\Lambda}$ between 0.7 and 1.5 GeV and show the predictions for all F and G waves in Figs. 4 and 5, respectively, in terms of shaded (colored) bands. It is seen that, at N³LO, the variations of the predictions are very large and always too attractive while, at N⁴LO, the variations are small and the predictions are close to the data or right on the data. Figs. 4 and 5 also include the lower orders (as defined in the Appendices) such that a comparison of the relative size of the order-by-order contributions is possible. We observe that there is not much of a convergence, since obviously the magnitudes of the NNLO, N³LO, and N⁴LO contributions are about the same. Potentially, this is characteristic for just these three orders and changes beyond N⁴LO. But only an explicit calculation at N⁵LO can settle this issue.

IV. CONCLUSIONS

In this paper, we have calculated the one- and two-loop 2 π -exchange (2PE) and two-loop 3 π -exchange (3PE) contributions to the NN interaction which occur at N⁴LO (fifth order) of the chiral low-momentum expansion. The calculations are based upon heavy-baryon chiral perturbation theory using the most general fourth order Lagrangian for pions and nucleons. We apply πN LECs, which were determined in an analysis of elastic pion-nucleon scattering to fourth order using the same power counting scheme as in the present work. The spectral functions, which determine the NN amplitudes via dispersion integrals, are regularized by a cutoff $\tilde{\Lambda}$ in the range 0.7 to 1.5 GeV (also known as spectral-function regularization). Besides the cutoff $\tilde{\Lambda}$, our calculations do not involve any adjustable parameters.

From past work on NN scattering in chiral perturbation theory (see, e.g., Ref. [15]), it is wellknown that, at NNLO and N³LO, chiral 2PE produces far too much attraction. The most important result of the present study is that the N⁴LO 2PE contributions are prevalingly repulsive and, thus, compensate the excessive attraction of the lower orders. As a consequence, the phase-shift predictions in F and G waves are in very good agreement with the data, with the only exception of the 1F_3 wave. The net 3PE contribution turns out to be moderate pointing towards convergence in terms of the number of pions exchanged between two nucleons. On the other hand, the NNLO, N³LO, and N⁴LO

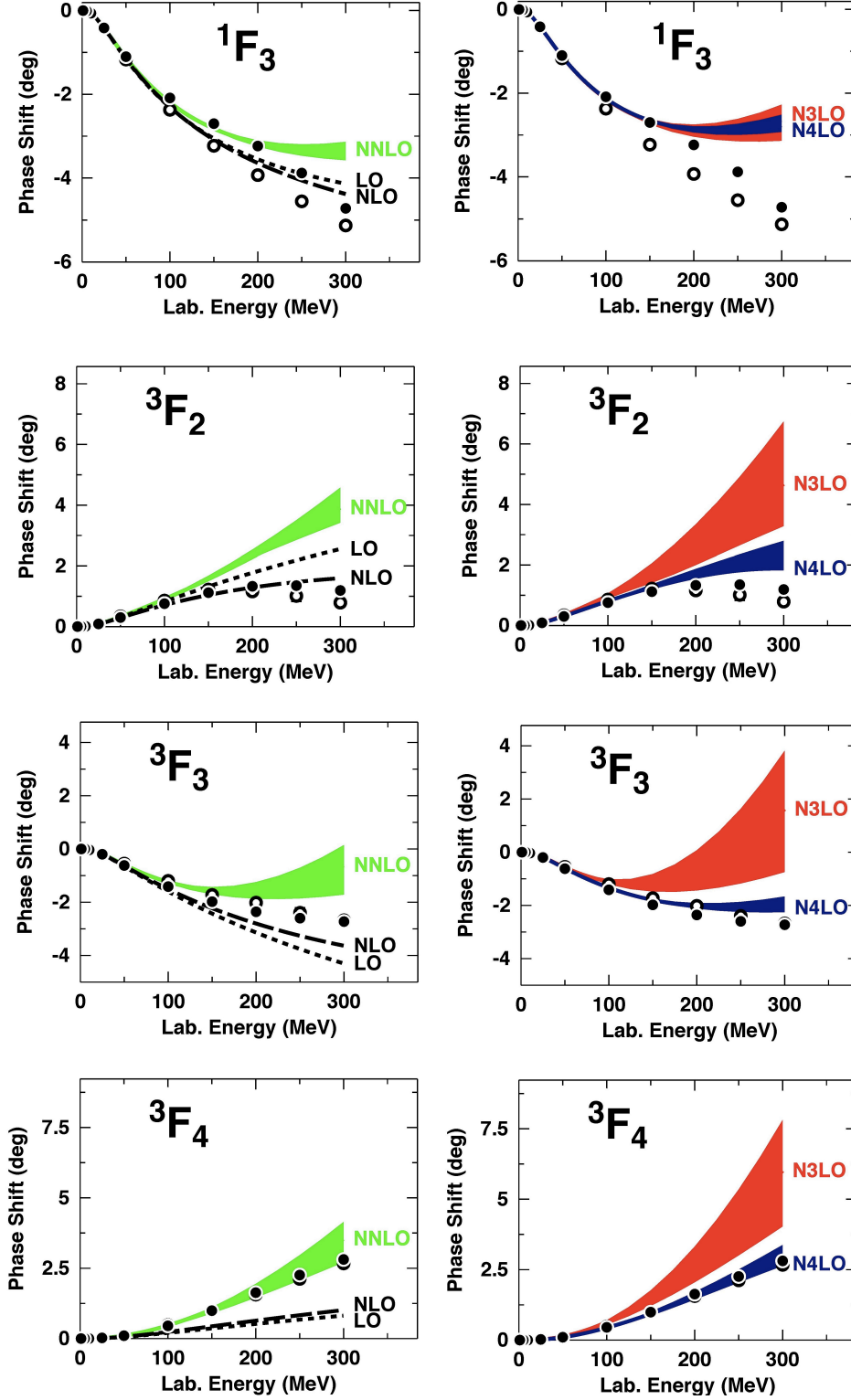


FIG. 4: (Color online) Phase-shifts of neutron-proton scattering at various orders as denoted. The shaded (colored) bands show the variation of the predictions when the SFR cutoff $\tilde{\Lambda}$ is changed over the range 0.7 to 1.5 GeV. The filled and open circles represent the results from the Nijmegen multi-energy np phase-shift analysis [33] and the VPI/GWU single-energy np analysis SM99 [34], respectively.

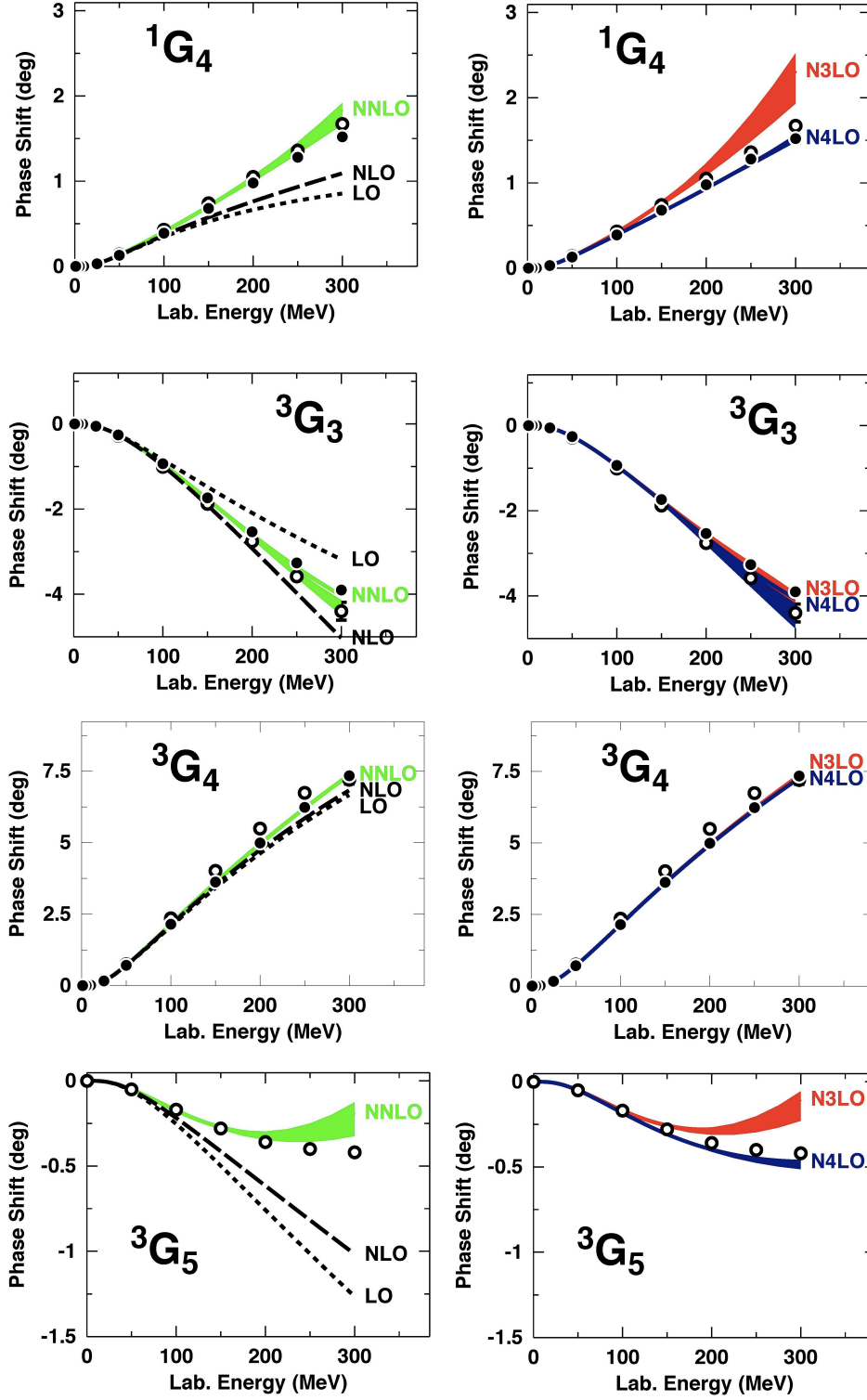


FIG. 5: (Color online) Same as Fig. 4, but for G -waves.

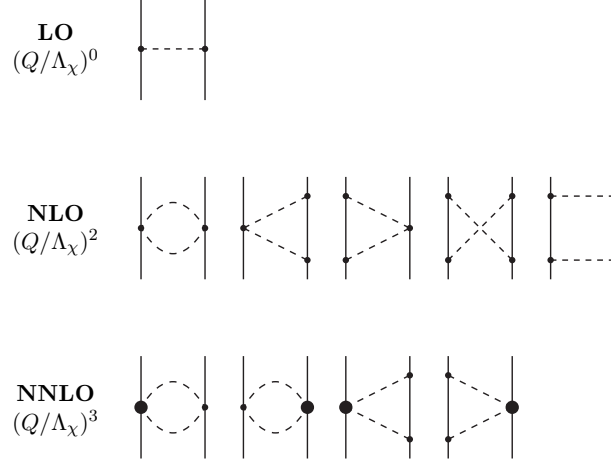


FIG. 6: LO, NLO, and NNLO contributions to the NN interaction. Notation as in Fig. 1.

contributions are all about the same magnitude raising some concern about the convergence of the chiral expansion of the NN amplitude. To obtain more insight into this issue, future investigations at $N^5\text{LO}$ may be necessary.

Acknowledgements

This work was supported in part by the U.S. Department of Energy under Grant No. DE-FG02-03ER41270 (R.M. and Y.N.), the Ministerio de Ciencia y Tecnología under Contract No. FPA2010-21750-C02-02 and the European Community-Research Infrastructure Integrating Activity “Study of Strongly Interacting Matter” (HadronPhysics3 Grant No. 283286) (D.R.E.), and by DFG and NSFC (CRC110) (N.K.).

Appendix A: Leading order

At leading order, there is only the 1π -exchange contribution, cf. Fig. 6. The charge-independent 1π -exchange is given by

$$V_{1\pi}^{(\text{CI})}(\vec{p}', \vec{p}) = -\frac{g_A^2}{4f_\pi^2} \boldsymbol{\tau}_1 \cdot \boldsymbol{\tau}_2 \frac{\vec{\sigma}_1 \cdot \vec{q} \vec{\sigma}_2 \cdot \vec{q}}{q^2 + m_\pi^2}. \quad (\text{A1})$$

Higher order corrections to the 1π -exchange are taken care of by mass and coupling constant renormalizations $g_A/f_\pi \rightarrow g_{\pi N}/M_N$. Note also that, on shell, there are no relativistic corrections. Thus, we apply 1π -exchange in the form Eq. (A1) through all orders.

In this paper, we are specifically calculating neutron-proton (np) scattering and take the charge-dependence of the 1π -exchange into account. Thus, the 1π -exchange potential that we actually apply reads

$$V_{1\pi}^{(np)}(\vec{p}', \vec{p}) = -V_{1\pi}(m_{\pi^0}) + (-1)^{I+1} 2V_{1\pi}(m_{\pi^\pm}), \quad (\text{A2})$$

where $I = 0, 1$ denotes the total isospin of the two-nucleon system and

$$V_{1\pi}(m_\pi) \equiv -\frac{g_A^2}{4f_\pi^2} \frac{\vec{\sigma}_1 \cdot \vec{q} \vec{\sigma}_2 \cdot \vec{q}}{q^2 + m_\pi^2}. \quad (\text{A3})$$

We use $m_{\pi^0} = 134.9766$ MeV and $m_{\pi^\pm} = 139.5702$ MeV. Formally speaking, the charge-dependence of the 1PE exchange is of order NLO [1], but we include it already at leading order to make the comparison with the np phase shifts more meaningful.

Appendix B: Next-to-leading order

The NN diagrams that occur at NLO (cf. Fig. 6) contribute in the following way [7]:

$$W_C = \frac{L(\tilde{\Lambda}; q)}{384\pi^2 f_\pi^4} \left[4m_\pi^2(1 + 4g_A^2 - 5g_A^4) + q^2(1 + 10g_A^2 - 23g_A^4) - \frac{48g_A^4 m_\pi^4}{w^2} \right], \quad (\text{B1})$$

$$V_T = -\frac{1}{q^2} V_S = -\frac{3g_A^4}{64\pi^2 f_\pi^4} L(\tilde{\Lambda}; q). \quad (\text{B2})$$

Appendix C: Next-to-next-to-leading order

The NNLO contribution (lower row of Fig. 6) is given by [7]:

$$V_C = \frac{3g_A^2}{16\pi f_\pi^4} [2m_\pi^2(c_3 - 2c_1) + c_3 q^2] (2m_\pi^2 + q^2) A(\tilde{\Lambda}; q), \quad (\text{C1})$$

$$W_T = -\frac{1}{q^2} W_S = -\frac{g_A^2}{32\pi f_\pi^4} c_4 w^2 A(\tilde{\Lambda}; q). \quad (\text{C2})$$

The loop function that appears in the above expressions, regularized by spectral-function cut-off $\tilde{\Lambda}$, is

$$A(\tilde{\Lambda}; q) = \frac{1}{2q} \arctan \frac{q(\tilde{\Lambda} - 2m_\pi)}{q^2 + 2\tilde{\Lambda}m_\pi}. \quad (\text{C3})$$

Note that

$$\lim_{\tilde{\Lambda} \rightarrow \infty} A(\tilde{\Lambda}; q) = \frac{1}{2q} \arctan \frac{q}{2m_\pi} \quad (\text{C4})$$

yields the loop function used in dimensional regularization.

Appendix D: Next-to-next-to-next-to-leading order

1. Football diagram at N³LO

The football diagram at N³LO, Fig. 7(a), generates [12]:

$$V_C = \frac{3}{16\pi^2 f_\pi^4} \left[\left(\frac{c_2}{6} w^2 + c_3(2m_\pi^2 + q^2) - 4c_1 m_\pi^2 \right)^2 + \frac{c_2^2}{45} w^4 \right] L(\tilde{\Lambda}; q), \quad (\text{D1})$$

$$W_T = -\frac{1}{q^2} W_S = \frac{c_4^2}{96\pi^2 f_\pi^4} w^2 L(\tilde{\Lambda}; q). \quad (\text{D2})$$

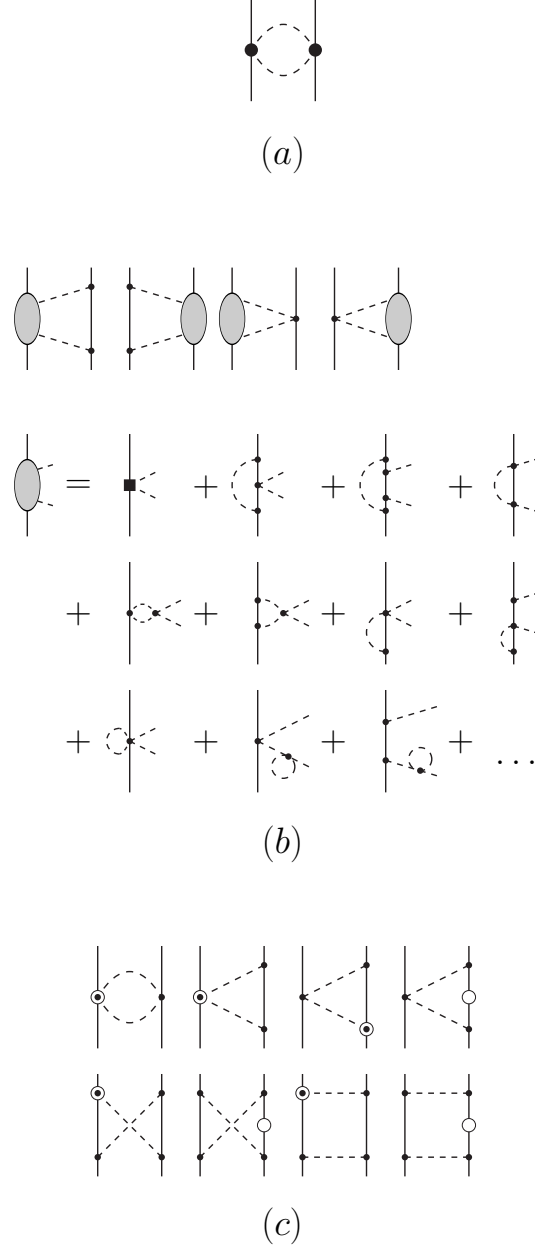


FIG. 7: Two-pion exchange contributions at $N^3\text{LO}$ with (a) the $N^3\text{LO}$ football diagram, (b) the leading 2PE two-loop contributions, and (c) the relativistic corrections of NLO diagrams. Notation as in Fig. 1.

2. Leading two-loop contributions

The leading order 2π -exchange two-loop diagrams are shown in Fig. 7(b). In terms of spectral functions, the results are [12]:

$$\text{Im } V_C = \frac{3g_A^4(2m_\pi^2 - \mu^2)}{\pi\mu(4f_\pi)^6} \left[(m_\pi^2 - 2\mu^2) \left(2m_\pi + \frac{2m_\pi^2 - \mu^2}{2\mu} \ln \frac{\mu + 2m_\pi}{\mu - 2m_\pi} \right) + 4g_A^2 m_\pi (2m_\pi^2 - \mu^2) \right], \quad (\text{D3})$$

$$\begin{aligned} \text{Im } W_C &= \frac{2\kappa}{3\mu(8\pi f_\pi^2)^3} \int_0^1 dx \left[g_A^2 (\mu^2 - 2m_\pi^2) + 2(1 - g_A^2) \kappa^2 x^2 \right] \\ &\times \left\{ 96\pi^2 f_\pi^2 [(2m_\pi^2 - \mu^2)(\bar{d}_1 + \bar{d}_2) - 2\kappa^2 x^2 \bar{d}_3 + 4m_\pi^2 \bar{d}_5] \right. \\ &+ [4m_\pi^2(1 + 2g_A^2) - \mu^2(1 + 5g_A^2)] \frac{\kappa}{\mu} \ln \frac{\mu + 2\kappa}{2m_\pi} + \frac{\mu^2}{12} (5 + 13g_A^2) - 2m_\pi^2(1 + 2g_A^2) \\ &- 3\kappa^2 x^2 + 6\kappa x \sqrt{m_\pi^2 + \kappa^2 x^2} \ln \frac{\kappa x + \sqrt{m_\pi^2 + \kappa^2 x^2}}{m_\pi} \\ &\left. + g_A^4 (\mu^2 - 2\kappa^2 x^2 - 2m_\pi^2) \left[\frac{5}{6} + \frac{m_\pi^2}{\kappa^2 x^2} - \left(1 + \frac{m_\pi^2}{\kappa^2 x^2} \right)^{3/2} \ln \frac{\kappa x + \sqrt{m_\pi^2 + \kappa^2 x^2}}{m_\pi} \right] \right\}, \quad (\text{D4}) \end{aligned}$$

$$\begin{aligned} \text{Im } V_S &= \mu^2 \text{Im } V_T = \frac{g_A^2 \mu \kappa^3}{8\pi f_\pi^4} (\bar{d}_{15} - \bar{d}_{14}) \\ &+ \frac{2g_A^6 \mu \kappa^3}{(8\pi f_\pi^2)^3} \int_0^1 dx (1 - x^2) \left[\frac{1}{6} - \frac{m_\pi^2}{\kappa^2 x^2} + \left(1 + \frac{m_\pi^2}{\kappa^2 x^2} \right)^{3/2} \ln \frac{\kappa x + \sqrt{m_\pi^2 + \kappa^2 x^2}}{m_\pi} \right], \quad (\text{D5}) \end{aligned}$$

$$\text{Im } W_S = \mu^2 \text{Im } W_T(i\mu) = \frac{g_A^4 (4m_\pi^2 - \mu^2)}{\pi(4f_\pi)^6} \left[\left(m_\pi^2 - \frac{\mu^2}{4} \right) \ln \frac{\mu + 2m_\pi}{\mu - 2m_\pi} + (1 + 2g_A^2) \mu m_\pi \right], \quad (\text{D6})$$

where $\kappa = \sqrt{\mu^2/4 - m_\pi^2}$.

The momentum space amplitudes $V_\alpha(q)$ and $W_\alpha(q)$ are obtained from the above expressions by means of the dispersion integrals shown in Eq. (2.11).

3. Leading relativistic corrections

The relativistic corrections of the NLO diagrams, which are shown in Fig. 7(c), count as N³LO and are given by [1]:

$$V_C = \frac{3g_A^4}{128\pi f_\pi^4 M_N} \left[\frac{m_\pi^5}{2\omega^2} + (2m_\pi^2 + q^2)(q^2 - m_\pi^2) A(\tilde{\Lambda}; q) \right], \quad (\text{D7})$$

$$W_C = \frac{g_A^2}{64\pi f_\pi^4 M_N} \left\{ \frac{3g_A^2 m_\pi^5}{2\omega^2} + [g_A^2(3m_\pi^2 + 2q^2) - 2m_\pi^2 - q^2] (2m_\pi^2 - q^2) A(\tilde{\Lambda}; q) \right\}, \quad (\text{D8})$$

$$V_T = -\frac{1}{q^2} V_S = \frac{3g_A^4}{256\pi f_\pi^4 M_N} (5m_\pi^2 + 2q^2) A(\tilde{\Lambda}; q), \quad (\text{D9})$$

$$W_T = -\frac{1}{q^2} W_S = \frac{g_A^2}{128\pi f_\pi^4 M_N} [g_A^2(3m_\pi^2 + q^2) - \omega^2] A(\tilde{\Lambda}; q), \quad (\text{D10})$$

$$V_{LS} = \frac{3g_A^4}{32\pi f_\pi^4 M_N} (2m_\pi^2 + q^2) A(\tilde{\Lambda}; q), \quad (\text{D11})$$

$$W_{LS} = \frac{g_A^2(1 - g_A^2)}{32\pi f_\pi^4 M_N} \omega^2 A(\tilde{\Lambda}; q). \quad (\text{D12})$$

4. Leading three-pion exchange contributions

The leading 3π -exchange contributions that occur at N³LO have been calculated in Refs. [9, 10] and are found to be negligible. We, therefore, omit them.

-
- [1] R. Machleidt and D. R. Entem, Phys. Rep. **503**, 1 (2011).
- [2] E. Epelbaum, H.-W. Hammer, and U.-G. Meißner, Rev. Mod. Phys. **81**, 1773 (2009).
- [3] J. Gasser and H. Leutwyler, Ann. Phys. (N.Y.) **158**, 142 (1984).
- [4] J. Gasser, M. E. Sainio, and A. Švarc, Nucl. Phys. **B307**, 779 (1988).
- [5] S. Weinberg, Phys. Lett **B251**, 288 (1990); Nucl. Phys. **B363**, 3 (1991).
- [6] C. Ordóñez, L. Ray, and U. van Kolck, Phys. Rev. Lett. **72**, 1982 (1994); Phys. Rev. C **53**, 2086 (1996).
- [7] N. Kaiser, R. Brockmann, and W. Weise, Nucl. Phys. **A625**, 758 (1997).
- [8] N. Kaiser, S. Gerstendörfer, and W. Weise, Nucl. Phys. **A637**, 395 (1998).
- [9] N. Kaiser, Phys. Rev. C **61**, 014003 (2000).
- [10] N. Kaiser, Phys. Rev. C **62**, 024001 (2000).
- [11] N. Kaiser, Phys. Rev. C **63**, 044010 (2001).
- [12] N. Kaiser, Phys. Rev. C **64**, 057001 (2001).
- [13] N. Kaiser, Phys. Rev. C **65**, 017001 (2002).
- [14] E. Epelbaum, W. Glöckle, and U.-G. Meißner, Nucl. Phys. **A637**, 107 (1998); **A671**, 295 (2000).
- [15] D. R. Entem and R. Machleidt, Phys. Rev. C **66**, 014002 (2002).
- [16] D. R. Entem and R. Machleidt, Phys. Rev. C **68**, 041001 (2003).
- [17] E. Epelbaum, W. Glöckle, and U.-G. Meißner, Nucl. Phys. **A747**, 362 (2005).
- [18] D. R. Entem, R. Machleidt, and H. Witala, Phys. Rev. C **65**, 064005 (2002).
- [19] M. Viviani, L. Girlanda, A. Kievsky, and L. E. Marcucci, Phys. Rev. Lett. **111**, 172302 (2013).
- [20] J. Golak *et al.*, arXiv:1410.0756 [nucl-th].
- [21] H. Krebs, A. Gasparyan, and E. Epelbaum, Phys. Rev. C **85**, 054006 (2012). We thank H. Krebs for pointing out and clarifying misprints in this paper.
- [22] H. Krebs, A. Gasparyan, and E. Epelbaum, Phys. Rev. C **87**, 054007 (2013).
- [23] L. Girlanda, A. Kievsky, M. Viviani, Phys. Rev. C **84**, 014001 (2011).
- [24] N. Fettes, U.-G. Meißner, and S. Steiniger, Nucl. Phys. A **640**, 199 (1998).
- [25] N. Fettes, U.-G. Meißner, M. Mojžiš, and S. Steininger, Ann. Phys. (N.Y.) **283**, 273 (2000); **288**, 249(E) (2001).
- [26] N. Fettes and U.-G. Meißner, Nucl. Phys. A **676**, 311 (2000).
- [27] E. Epelbaum, W. Glöckle, and U.-G. Meißner, Eur. Phys. J. A **19**, 125 (2004).
- [28] G. Q. Li and R. Machleidt, Phys. Rev. C **58** (1998) 3153.
- [29] K. Erkelenz, R. Alzetta, and K. Holinde, Nucl. Phys. **A176**, 413 (1971); note that there is an error in equation (4.22) of this paper where it should read
- $${}^{-}W_{LS}^J = 2qq' \frac{J-1}{2J-1} \left[A_{LS}^{J-2,(0)} - A_{LS}^{J(0)} \right]$$
- and
- $${}^{+}W_{LS}^J = 2qq' \frac{J+2}{2J+3} \left[A_{LS}^{J+2,(0)} - A_{LS}^{J(0)} \right].$$
- [30] R. Machleidt, in: *Computational Nuclear Physics 2 – Nuclear Reactions*, edited by K. Langanke, J.A. Maruhn, and S.E. Koonin (Springer, New York, 1993) p. 1.
- [31] R. Machleidt, Phys. Rev. C **63** 024001 (2001).
- [32] H. P. Stapp, T. J. Ypsilantis, and N. Metropolis, Phys. Rev. **105**, 302 (1957).
- [33] V. G. J. Stoks, R. A. M. Klomp, M. C. M. Rentmeester, and J. J. de Swart, Phys. Rev. C **48**, 792 (1993).
- [34] R. A. Arndt, I. I. Strakovsky, and R. L. Workman, SAID, Scattering Analysis Interactive Dial-in computer facility, George Washington University (formerly Virginia Polytechnic Institute), solution SM99 (Summer 1999); for more information see, e. g., R. A. Arndt, I. I. Strakovsky, and R. L. Workman, Phys. Rev. C **50**, 2731 (1994).
- [35] A. D. Jackson, D. O. Riska, and B. Verwest, Nucl. Phys. **A249**, 397 (1975).
- [36] G. E. Brown and A. D. Jackson, *The Nucleon-Nucleon Interaction* (North-Holland, Amsterdam, 1976).
- [37] R. Vinh Mau, in: *Mesons in Nuclei*, Vol. I, edited by M. Rho and D. H. Wilkinson (North-Holland, Amsterdam, 1979), p. 151.
- [38] M. Lacombe, B. Loiseau, J. M. Richard, R. Vinh Mau, J. Côté, P. Pires, and R. de Tourreil, Phys. Rev. C **21**, 861 (1980).